

Sparse Uncertainty-Informed Sampling from Federated Streaming Data

Manuel Röder^{1,2,3} and Frank-Michael Schleif¹ *

1 - Technical UAS Würzburg-Schweinfurt, Fac. of Computer Science, Würzburg, DE

2 - Bielefeld University, Faculty of Technology, Bielefeld, DE

3 - Center for Artificial Intelligence and Robotics, Würzburg, DE

Abstract. We present a numerically robust, computationally efficient approach for non-I.I.D. data stream sampling in federated client systems, where resources are limited and labeled data for local model adaptation is sparse and expensive. The proposed method identifies relevant stream observations to optimize the underlying client model, given a local labeling budget, and performs instantaneous labeling decisions without relying on any memory buffering strategies. Our experiments show enhanced training batch diversity and an improved numerical robustness of the proposal compared to existing strategies over large-scale data streams, making our approach an effective and convenient solution in FL environments.

1 Introduction

The rapid evolution of digital technologies and the exponential growth of data, coupled with the society’s increased demand for data protection, have underscored the significant importance of *Federated Learning* (**FL**) [1] in the modern AI era. This innovative approach to machine learning embodies the shift towards decentralised data processing that preserves privacy and enables collaborative learning without direct data exchange. The relevance of FL extends across a wide range of sectors, particularly where data protection, real-time analytics and security are crucial, such as healthcare, finance, automotive and manufacturing [2, 3, 4]. The necessary extension of FL to *streaming data* [5] in this context poses new challenges due to its real-time nature and source variability, demanding instant decision making and model adaptation in high-volume data processing pipelines that operate under resource constraints [6]. Given the voluminous nature of data streams and the high costs of data labeling, it is impractical and inefficient to process every data point for model training. Selective sampling plays a critical role in addressing this issue by identifying and selecting the most beneficial data points for model updates, thereby optimising the learning process. In general, one key challenge is to develop mechanisms that can perform this selection accurately and rationally in real-time, while remaining numerically stable despite iterating over thousands of data points. Efficiently determining which data points warrant expert labeling becomes a pivotal aspect of the learning process, particularly in scenarios where labeled data is scarce or costly to acquire. The ability to strategically focus expert intervention on the most impactful data points is extensively researched in the field of *Active Learning* [7] and can significantly accelerate the learning process and enhance the overall effectiveness of the FL system.

*MR is supported through the Bavarian HighTech Agenda, specifically by the Würzburg Center for Artificial Intelligence and Robotics (CAIRO) and the ProPere THWS scholarship.

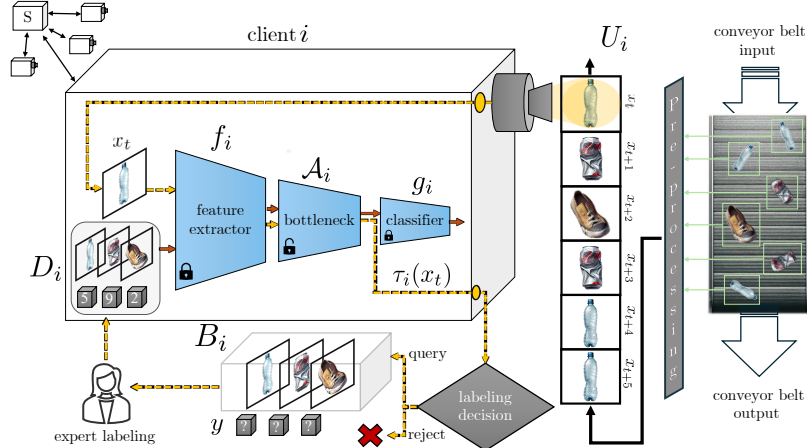


Fig. 1: Sparse sample selection from federated streaming data, exemplified by conveyor belt object scanning on client i : the orange, dashed data flow illustrates the decision-making algorithm; the red data flow depicts the fine-tuning pipeline.

In this study, we introduce an advanced method that empowers resource-limited FL clients to select the most valuable samples to refine their neural network models from streaming data in real-time. This approach prioritizes resource efficiency and numerical stability. To achieve this, we employ a query strategy derived from *Volume Sampling for Streaming Active Learning* [8], which makes labeling choices based on the penultimate layer representations, within a conformal FL framework. We modify this strategy for the FL streaming context by substituting the iterative Woodbury Identity update mechanism [9] – which adjusts sampling probabilities – with low-rank updates to the lower Cholesky triangular matrix [10]. This modification simplifies the decision process and ensures numerical stability across a vast array of streamed data points.

2 Methodology

2.1 Setup and Prerequisites

We consider a FL environment characterized by a central, resource-rich server S tasked with network orchestration and multiple resource-limited clients indexed by i , where $i = 1, \dots, I$ as outlined in Fig. 1. Clients operate without long-term storage, demanding immediate labeling decisions - a unique challenge. The client model features a core sequence of three components, including a pre-trained feature extractor $f(\cdot)$, a bottleneck module $\mathcal{A}(\psi)$, and a linear classification head $g(\cdot)$. Given an input sample x observed on client i , the overall decision function is then expressed as $\mathcal{F}_i(x) = g(\mathcal{A}_{\psi_i}(f(x)))$. This configuration is aligned with (but not limited to) the principles outlined in FedAcross [11], a scalable FL framework designed to handle client adaptation tasks with scarcely labeled target data. Furthermore, the client i inspects sample x_t , seen only once, from the *non-I.I.D.* data stream U_i at time t , in which the occurrence of objects is

not evenly distributed, using an arbitrary sensing device. To address the high labeling costs and limited resources for a single round of FL on a client edge device, we introduce a labeling budget k that limits the set of selected samples B_i , such that $|B_i| \leq k$ applies. After exhausting the labeling budget k in the current FL round, we obtain labels for all samples in B_i from an oracle and refine the client model by optimizing the cross-entropy loss between $\mathcal{F}_i(\cdot)$'s output and the acquired labels.

Main contributions: We provide an efficient sampling strategy that performs an instant decision about current stream sample x_t being included in B_i or not whilst *a)* sticking to the labeling budget k to address local resource constraints, *b)* enforcing batch diversity over all samples within B_i to maximize training efficiency of the underlying client model and *c)* keeping the algorithmic response stable and immediate over a large number of iterative processing steps to enable unsupervised stream observation over extended time periods.

2.2 Algorithm

The proposed algorithm for deciding whether or not to request a label for sample x_t on client i performs an uncertainty measure on its representation in the embedding space of the penultimate layer of the underlying model. Therefore, the employed embedding function is defined over the client-side feature extractor f_i and the bottleneck layer \mathcal{A}_i using $\tau_i(x_t) = \mathcal{A}_i(f_i(x_t))$, $\tau_i(x_t) \in \mathbb{R}^d$, with d defining the output dimension of the penultimate network layer. Our method follows the volume sampling technique proposed in [8] by choosing a sample x_t for labeling with a probability p , proportional to its gradient's determinantal contribution. Assuming that the underlying client data distribution is non-stationary, the probability p_t is then computed to adhere for the streaming setting with

$$p_t = \frac{q_t \cdot \tau_i(x_t)^T \hat{\Sigma}_t^{-1} \tau_i(x_t)}{\text{tr} \left(\frac{1}{t} \hat{\Sigma}_t^{-1} \sum_{i=1}^t \tau_i(x_t) \tau_i(x_t)^T \right)}, \quad (1)$$

where $\hat{\Sigma}_t^{-1}$ denotes the inverse of the tracking covariance matrix $\mathbf{A}_t \in \mathbb{R}^{d \times d}$ over samples already included in B_i and q_t refers to the adaptive labeling frequency for the current stream observation defined as $q_t = (k - |B_i|) / (|U_i| - t)$.

To effectively update and inverse \mathbf{A} for each new sample in the limited-resource regime of a federated client, we employ a *Cholesky decomposition-based low-rank update mechanism* [10]. We argue that alternative solutions driven by Sherman-Morrison-Woodbury formula to update the tracking covariance matrix after positive rank-1 updates suffer from numerical instabilities, rendering it impractical for large-scale stream sampling in industrial applications.

Hence, for $t = 0$, the algorithm initializes the lower triangular matrix \mathbf{L}_t by calculating the Cholesky decomposition of the (symmetric, positive-definite) tracking covariance matrix \mathbf{A}_t with $\mathbf{A}_t = \mathbf{L}_t \mathbf{L}_t^T$. After determination by Equation (1) that the currently observed sample x_t is eligible to be included in B_i , the updated inverse of the tracking covariance matrix $\hat{\Sigma}_{t+1}^{-1}$ is obtained in two steps: First, the algorithm performs a positive rank-1 update by adding the sample's embedded representation $\tau_i(x_t)$ to the Cholesky factor \mathbf{L}_t with

$$\mathbf{L}_{t+1} = \mathbf{L}_t + \tau_i(x_t) (\tau_i(x_t))^T. \quad (2)$$

Noting that Equation (2) can be re-written to

$$\mathbf{L}_{t+1} = \begin{bmatrix} \mathbf{L}_t^T \\ \tau_i(x_t)^T \end{bmatrix}^T \begin{bmatrix} \mathbf{L}_t^T \\ \tau_i(x_t)^T \end{bmatrix}, \quad \mathbf{Q}^T \begin{bmatrix} \mathbf{L}_t^T \\ \tau_i(x_t)^T \end{bmatrix} = \begin{bmatrix} \mathbf{L}_{t+1} \\ 0 \end{bmatrix} \quad (3)$$

this problem can be efficiently computed as a product of *Givens* rotations $\mathbf{Q} = \mathbf{Q}_1 \cdots \mathbf{Q}_n$, see [12]. Taking advantage of the retained lower triangular structure of \mathbf{L}_{t+1} , the second step to refactor $\hat{\Sigma}_{t+1}^{-1}$ involves calculating the inverse of the updated Cholesky factor using $\hat{\Sigma}_{t+1}^{-1} = (\mathbf{L}_{t+1}(\mathbf{L}_{t+1})^T)^{-1}$, which can be solved efficiently by employing an algorithm based on repeated back-substitutions [10]. Subsequently, after having observed all elements of U_i , domain expert labeling is queried for selected samples in B_i and the labeled batch is added to the training data set D_i for model adaptation on client i . A pseudocode is given in Alg. 1.

Algorithm 1 Federated Stream Sampling

Require: Embedding function $\tau_i(x) = \mathcal{A}_i(f_i(x))$ on client i , unlabeled stream of samples U_i , adaptive sampling rate q , labeling budget k

- 1: Initialize $t = 1$, $\hat{\Sigma}_0^{-1} = \lambda^{-1}\mathbf{I}_d$ ▷ regularized by λ for stability
- 2: Initialize $\mathbf{A}_0 = \mathbf{0}_{d,d}$ ▷ covariance over all data
- 3: Initialize $B_i = \{\}$ with $|B_i| \leq k$ upon additions ▷ limit selected samples
- 4: Initialize $\mathbf{L}_0 = \text{CHOL}(\mathbf{A}_0)$ ▷ Cholesky lower triangular factorization
- 5: **for** $x_t \in U_i$ **do**
- 6: $\mathbf{A}_t \leftarrow \frac{t-1}{t}\mathbf{A}_{t-1} + \frac{1}{t}\tau_i(x_t)\tau_i(x_t)^T$ ▷ covariance matrix update
- 7: $p_t = q \cdot \tau_i(x_t)^T \hat{\Sigma}_t^{-1} \tau_i(x_t) \text{tr}(\hat{\Sigma}_t^{-1} \mathbf{A}_t)^{-1}$ ▷ sampling prob. according to Eq. (1)
- 8: **with probability** $\min(p_t, 1)$:
- 9: $B_i \leftarrow B_i \cup \{x_t\}$
- 10: $\mathbf{L}_{t+1} \leftarrow \text{CHOLUPDATE_LOW_RANK}(\mathbf{L}_t, \tau_i(x_t))$ ▷ update according to Eq. (3)
- 11: $\hat{\Sigma}_{t+1}^{-1} \leftarrow (\mathbf{L}_{t+1}(\mathbf{L}_{t+1})^T)^{-1}$
- 12: **else:**
- 13: $\hat{\Sigma}_{t+1}^{-1} \leftarrow \hat{\Sigma}_t^{-1}$
- 14: **end for**
- 15: $\text{QUERY_LABELS}(B_i)$ ▷ request domain expert labeling
- 16: **return** labeled batch B_i for client i model adaptation

3 Experiments

To highlight our sampling strategy’s benefits for large-scale federated streaming data, we evaluate three key aspects: **numerical stability**, **wall-clock runtime**, and **sampling quality** in the following experiments, mimicking real-world scenarios on resource-constrained FL clients.

The *first experiment* examines the low-rank update mechanism that iteratively recomputes the inverse tracking covariance matrix $\hat{\Sigma}^{-1}$ after adding a new sample to B in regards to its numerical stability over a large number of update cycles. We therefore measure the reconstruction quality by means of relative error between the directly computed matrix \mathbf{A}_{dir} , updated by a randomized vector $\mathbf{v} \in \mathbb{R}^d$ such that $\mathbf{A}_{dir} = (\mathbf{A} + \mathbf{v}\mathbf{v}^T)^{-1}$, and the corresponding matrices calculated employing low-rank update strategies based on both Woodbury formula \mathbf{A}_{wbf} and Cholesky decomposition \mathbf{A}_{cho} (ours). The relative error is subsequently

defined as $\|\mathbf{A}_{wbf} - \mathbf{A}_{dir}\|_F / \|\mathbf{A}_{dir}\|_F$ and $\|\mathbf{A}_{cho} - \mathbf{A}_{dir}\|_F / \|\mathbf{A}_{dir}\|_F$, with $\|\cdot\|_F$ employing the Frobenius norm. The results of this experiment, traced over 1000 iterative updates with input dimensions $d \in \{256, 1024, 2048\}$, are shown in Fig. 2. The experiment demonstrates that our approach achieves faster convergence to a stable error and maintains consistently low relative reconstruction error rates throughout the iterative process across all input dimensions, in comparison to the Woodbury update-based method. It is important to note that, unlike our technique, the Woodbury update-based method becomes unstable at higher input dimensions (see fluctuation for $d = 2048$), underlining the future-proof suitability of our method for ever-increasing neural network models.

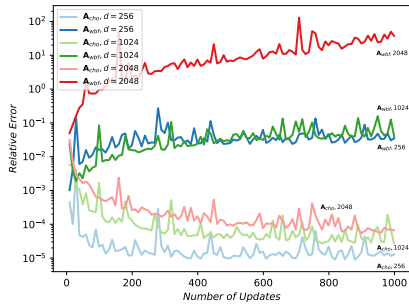


Fig. 2: Relative matrix reconstruction error comparison.

Method	Complexity	d	$\bar{\mathcal{O}}$ Time sec $\times 10^{-3}$
Direct	$\mathcal{O}(d^3)$	256	0.76 ± 0.53
		1024	16.11 ± 3.65
		2048	111.86 ± 14.36
Woodbury	$\mathcal{O}(r^2d)$	256	0.60 ± 0.50
		1024	10.96 ± 2.52
		2048	86.55 ± 13.63
Ours	$\mathcal{O}(\frac{1}{3}d^3)$	256	0.60 ± 0.49
		1024	6.68 ± 1.54
		2048	45.05 ± 6.47

Fig. 3: Algorithmic complexity and average wall-clock runtime comparison. Results calculated over three runs.

In the *second experiment* we evaluate our approach in terms of practical wall clock computation times on a CPU-based system. Simulating a low-resource edge device without access to GPU acceleration, we follow exactly the same setup as explored in the first experiment. The computation times are averaged for each dimension over the number of update cycles, see Fig. 3. Although Woodbury updates (rank $r=1$) have lower theoretical operation counts than Cholesky-based low-rank techniques, they do not consider the nature of the calculations, granting our method a significant advantage in practical implementations: Our approach operates exclusively on lower triangular forms, using cheap back-substitutions and avoiding complex operations for zero elements of the matrix. This results in compute times that are on-par or faster in all scenarios.

The *third experiment* visually confirms that our approach produces high-quality samples that can significantly contribute to model training optimization. In this setup, the (client) model is first fine-tuned on CIFAR-10 training data as described in [11]. The stream sampling is subsequently performed with our see-only-once-strategy over the held-back test set of 10,000 images, cast as non-I.I.D. data stream under artificial feature drift as outlined in [8], with a labeling bud-

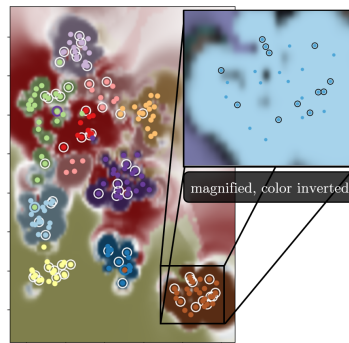


Fig. 4: Model decision regions.

get $k = 60$. We depict the model’s decision regions and our selected data points (highlighted white circles) with DeepView [13] after adding randomly chosen samples for better illustration in Fig. 4. DeepView visualizes neural networks’ decision functions in 2D by applying discriminative dimensionality reduction, thus revealing how our model classifies data. DeepView’s reliability stems from its focus on features crucial for decision-making, offering precise insights into a model’s behavior. The plot confirms on the one hand that the sampling mass is well-distributed across the data stream by delivering a class-diversified batch B and on the other hand that the decision-making algorithm tends to choose samples living near the edge of the model’s decision boundaries (see color-inverted, magnified area), providing relevant information for the training process.

4 Conclusion

In this work, we introduced a novel sampling strategy for federated streaming data, driven by a decision making engine that iteratively performs low-rank updates on the Cholesky factor, efficiently recalculating the inverse covariance matrix which is employed to evaluate model training importance of an observation instantly. The experimental results demonstrate that our method not only ensures numerical stability by reducing the accumulation of round-off errors over a large number of sampling iterations, but also minimizes computational overhead and enhances real-time system performance while selecting high-quality data points to support and improve model adaptation on federated clients.

Future work might explore methods to leverage the expert-labeled samples not only in the scope of local client personalization, but also for global FL model enhancements. *Code available at* github.com/cairo-thws/fed_streaming.

References

- [1] B. McMahan et al. Communication-efficient learning of deep networks from decentralized data. In *Proc. 20th AISTAT*, volume 54, pages 1273–1282, April 2017.
- [2] N. Rieke. The future of digital health with federated learn. *Digital Medicine*, 3, 12 2020.
- [3] G. Long et al. Federated learning for open banking. In *Fed. Learn. - Privacy and Incentive*, volume 12500 of *LNCIS*, pages 240–254. Springer, 2020.
- [4] H. Zhang et al. End-to-end federated learning for autonomous driving vehicles. In *2021 IJCNN*, pages 1–8, 2021.
- [5] M. Heusinger. *Learning with high dimensional data and preprocessing in non-stationary environments*. PhD thesis, Bielefeld University, Germany, 2023.
- [6] O. Marfoq et al. Federated learning for data streams. In *Proc. 26th AISTAT*, volume 206, pages 8889–8924. PMLR, 25–27 Apr 2023.
- [7] B. Settles. Active learning literature survey. CS Tech. Rep. 1648, WISC, 2009.
- [8] A. Saran et al. Streaming active learning with deep neural networks. In *Proc. 40th ICML, ICML’23*. JMLR.org, 2023.
- [9] M. Woodbury. Inverting modified matrices. In *Mem. Rept. 42*, page 4. Princeton, 1950.
- [10] M. Seeger. Low rank updates for the cholesky decomposition. 2004.
- [11] M. Röder et al. Crossing Domain Borders with Federated Few-Shot Adaptation. In *Proc. 13th ICPHAM*, pages 511–521, 2024.
- [12] G. Golub et al. *Matrix Computations*, pages 338–341. JHU Press, 20134.
- [13] A. Schulz et al. Deepview: Visualizing classification boundaries of deep neural networks as scatter plots using discriminative dimensionality reduction. In *Proc., IJCAI 2020*, pages 2305–2311. ijcai.org, 2020.